Diamond Detector Technology: Status and Perspectives

Michael Reichmann[*][†]

Eidgenoessische Technische Hochschule Zuerich (CH)

E-mail: `michael.reichmann@cern.ch`

Here could be your abstract ;-)

---

[*]Speaker.
[†]The full list of RD42 authors is provided in the appendix.

1. Introduction

The upgrade of the Large Hadron Collider (LHC) to the High Luminosity LHC (HL-LHC) from 2023 to 2025 [1] will push the luminosity limits even above the original design values of the LHC and will therefore hopefully give us even more insights in the fundamental nature of the universe. In 2028 an instantaneous luminosity of $5 \times 10^{34}\,\mathrm{cm}^{-2}\,\mathrm{s}^{-1}$ is aspired. This will be equivalent to a fluence of $2 \times 10^{16}\,\mathrm{n_{eq}/cm^2}$ [2] for the innermost tracking layer at a distance of $\sim 30\,\mathrm{mm}$ from the interaction point. In this environment, pixel hit rates of $3\,\mathrm{GHz/cm^2}$ are expected. The current pixel detectors are designed to withstand $\sim 300\,\mathrm{fb}^{-1}$ and thus the full detector would have to be replaced about every semester. This fact led to research and development of various radiation hard detector designs and materials.

Its large displacement energy and a high band gap of $5.5\,\mathrm{eV}$ at $305\,\mathrm{K}$ make diamond an excellent candidate for such a radiation tolerant detector which is why the RD42 Collaboration is investigating single-crystal (sc) and poly-crystalline (p) Chemical Vapour Deposition (CVD) diamond as an alternative for precision tracking detectors for over two decades. In order to grow high quality detector grade diamonds, RD42 collaborates with industrial companies. All shown results are acquired with scCVD diamonds produced by Element Six Technologies [9] and pCVD diamonds produced by II-VI Incorporated [11]. The two companies use propriety CVD processes to fabricate their products. Both diamond types are grown on homo-epitaxial substrates with the difference that for scCVD another scCVD diamond is used as substrate and thus its size is limited to $\sim 0.25\,\mathrm{cm^2}$. However, for the pCVD a diamond powder can be used as a substrate whereby it can be grown to wafers of diameters up to 6 inch [4]. In various studies it was found out that compared to corresponding silicon detectors, diamond is at minimum three times more radiation hard [7], has at least a two times faster charge collection [12] and its thermal conductivity is four times higher [13].

Due to the very high particle fluxes and radiation doses expected for the HL-LHC it is very important to understand the behaviour of future detectors in this environment. The RD42 Collaboration has studied CVD diamond detectors with irradiation doses up to $2.2 \times 10^{16}\,\mathrm{p/cm^2}$. In order to build even more radiation hard detectors a new technology - 3D detectors [3] - is investigated. The clever design of these detectors allows to heavily reduce the drift distance of the created charge carriers without reducing the total number of the created electron-hole pairs. Since the the signal behaviour of diamonds at high fluxes is uncertain, high rate studies are performed at Paul Scherrer Institut (PSI) with nearly minimum ionising particles (MIPs) and tunable particle fluxes from the order of $1\,\mathrm{kHz/cm^2}$ up to the order of $10\,\mathrm{MHz/cm^2}$.

2. Diamond Detectors at CERN

It is essential for all modern collider experiments to have an online monitoring of the beam conditions. Since it is important to have these detectors as close as possible to the beam all of the four main experiments at the LHC are using detectors with diamond sensors. ATLAS [10], ALICE, CMS [5] and LHCb [8] all make use of various Beam Condition Monitors (BCMs) and/or Beam Loss Monitors (BLMs) based on both CVD type diamonds for live background estimations and luminosity measurements.

As an upgrade of the BCM during the long shutdown in 2014 ATLAS installed the Diamond Beam

Monitor (DBM). Its purpose is to measure an instantaneous (bunch-by-bunch) luminosity and the bunch-by-bunch position of the beam spot. With its eight telescopes à three detector planes it adds tracking capability to the existing precise time-of-flight (ToF) measurements of the eight pad detectors of the BCM. The usage of state of the art pixel detectors based on the FE-I4b readout chip strongly increases the spatial resolution of the monitor and due to its projective geometry pointing towards the interaction region it also can distinguish particles coming from collisions and background [6]. The telescopes whereof the sensors of two are made out silicon and the other six out of pCVD diamond are positioned symmetrically around the beam pipe on both sides of the interaction point (IP) and are shown in figure 1. A total number of 45 diamonds with a thickness of 500 μm was available for the project of which the best for chosen for the detector.
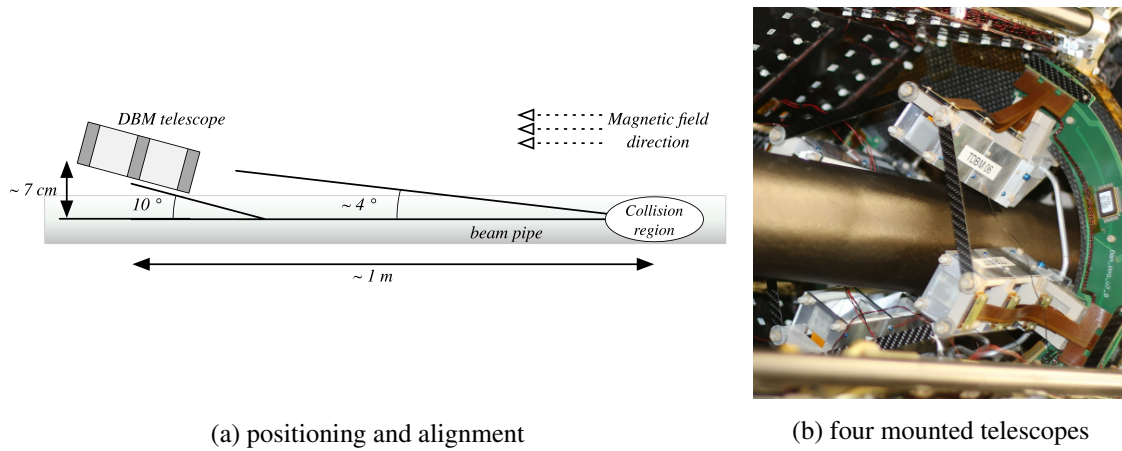

(a) positioning and alignment

(b) four mounted telescopes

Figure 1: DBM telescope

Shortly after the installation some of the modules broke (both silicon and diamond)and the DBM became non-operational. Nevertheless the first results already look promising as the plots in figure 2 proof. They show a clear discrimination between collision and background events. During the shutdown of the LHC in the beginning of 2017 the surviving modules were successfully recommissioned and became now a part of the ATLAS data taking.
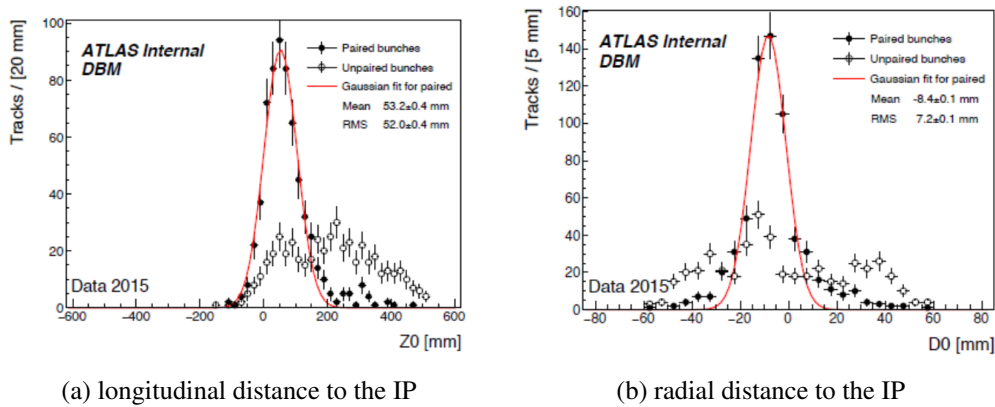

(a) longitudinal distance to the IP

(b) radial distance to the IP

Figure 2: Reconstruction of tracks from three modules using the initial alignment.

Du to the increasing particle fluence and excellent properties it is likely that diamond detectors become more popularin the future. The current research concentrates on 3D diamond detectors which will be described in section 5 on page 6 as a possible candidate for the innermost tracking detectors of the LHC. But there is also work towards an upgrade of the BCM to the BCM' which is designed to provide a fast (bunch-by-bunch) abort system for ATLAS as well as precise luminosity measurement for the HL-LHC.
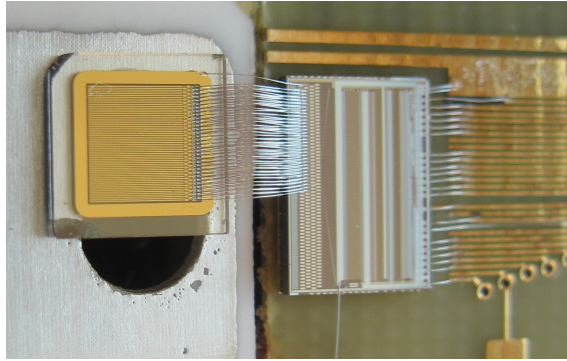
3. Radiation Tolerance

In order to probe the radiation tolerance of CVD diamond sensors several radiation studies have been performed varying the types and energies of damaging particles. The sensors were irradiated with protons with energies of 24 GeV, 800 MeV, 70 MeV and 25 MeV, 1 MeV neutrons and 200 MeV pions up to a maximum dose of 2.2×10^{16} p/cm^2 which is equivalent to ∼500 Mrad.

3.1 Preparation of the Detector

In a first step the surface of the raw diamond sensor has to be polished, cleaned and prepared for photo-lithography. Using the photo-lithography a metallisation pattern is then brought on the surface of the diamond. Depending on the pattern three types of detectors can be created: pad, strip and pixel detectors. This process is done for both of the sides of the diamond sensor whereby an almost edgeless design is obtained. By using a segmentation of the detector one can probe the charge of the detector depending on the position of the sensor which is critical for radiation studies. In this case solely strip detectors were used which were then mounted and connected to an amplifier to read out the charge of each strip. An image of the metallisation pattern and an example of a final detector are shown in figure 3.
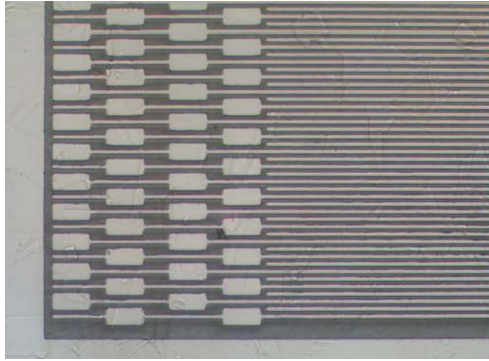
(a) Strip metallisation pattern   (b) A mounted diamond detector with amplifier

Figure 3: Detector for radiation studies

3.2 Setup

The characterisation of the irradiated devices was performed at the Super Proton Synchrotron (SPS) beam line at CERN with MIPs with momenta of the order of 100 GeV/c. By using a customised beam telescope with a spacial resolution of ∼2 μm one obtains an unbiased or transparent

hit prediction of the particle track in the diamond sensor. The schematic setup is shown in figure 4. Two pairs of crossing silicon strip detectors are positioned equally spaced in front and after the device under test (DUT). At the end of the telescope is a scintillator as reference.
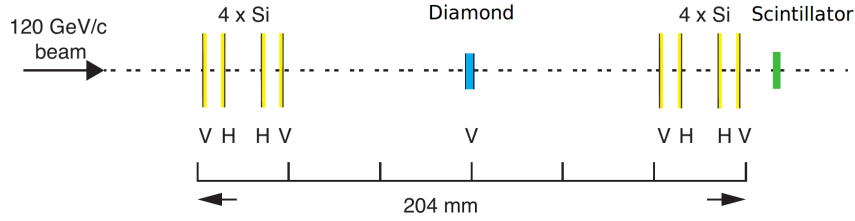

Figure 4: Schematic beam test setup

3.3 Results

The signal behaviour of irradiated material follows the simple damage equation where n_0 is

$$n = n_0 + k\phi \tag{3.1}$$

$$\frac{1}{\text{mfp}} = \frac{1}{\text{mfp}_0} + k\phi \tag{3.2}$$

the initial number of traps, mfp_0 is the initial mean free path (MFP), k a damage constant and ϕ the fluence. Since the measurable quantity is the charge collection distance (CCD) we have to find a relation to the mean free path. The CCD is the average distance between an electron-hole pair until it is trapped. For a scCVD diamond it is about the same size as the its thickness, for the pCVD the CCD is in general smaller than the thickness. In order to find the relation between CCD and MFP we have to correct our data with some simple assumptions like taking the same MFP for electrons and holes. This relates to the following equation:

$$\frac{\text{ccd}}{t} = \sum_i \frac{\text{mfp}_i}{t} \left(1 - \frac{\text{mfp}_i}{t} \left(1 - e^{-\frac{t}{\text{mfp}_i}} \right) \right) \tag{3.3}$$

The results of two different types of irradiation are shown in figure 5 on the next page. As seen in the examples all of the tested samples follow the equation 3.2. Table 1 on the next page shows all the extracted damage constants. As expected neutrons and low energy protons create the biggest damage in the material.

4. Rate Studies

In addition to the radiation studies it is also very important to understand the signal behaviour of CVD diamonds depending on the incident particle flux since the HL-LHC will reach values in the low GHz/cm^2 range. In order to conduct such a study it is import to have the possibility to vary the particle flux in big range. The πM1 beam line at the High Intensity Proton Accelerator (HIPA) at PSI provides such an environment. It has a π^+ beam with a spacing of 19.8 ns between the bunches
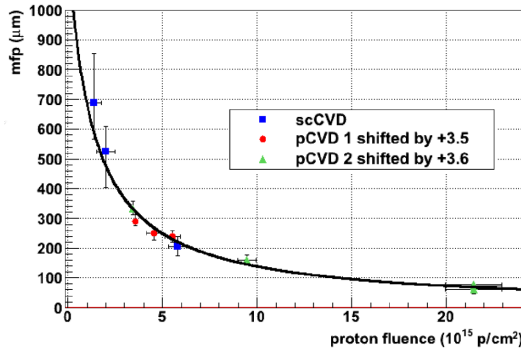
(a) 24 GeV protons at CERN PS
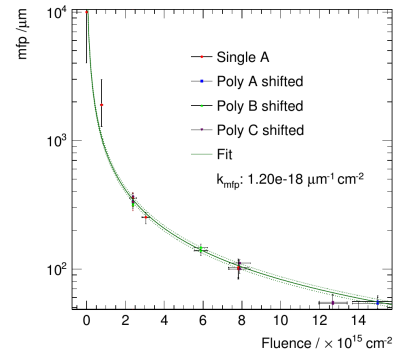
(b) 800 MeV protons at LANL

Figure 5: Irradiation results

Particle	Energy	Relative k
Proton	24 GeV	1.0
	800 MeV	1.79 ± 0.13
	70 MeV	2.4 ± 0.4
	25 MeV	4.5 ± 0.6
Neutron	1 MeV	4.5 ± 0.5
Pion	200 MeV	$2.5 - 3$

Table 1: Relative damage constants for various irradiation types

with continuously tunable particle fluxes from the order of $1\,\mathrm{kHz/cm^2}$ up to $10\,\mathrm{MHz/cm^2}$. The pion momentum of $260\,\mathrm{MeV/c}$ was chosen in order to reach the highest possible flux.

The diamond sensors were measured in a pad geometry and prepared in the same fashion described in section 3 on page 3. They have a size of approximately $4\,\mathrm{mm} \times 4\,\mathrm{mm}$ with a chrome-gold metalisation of $3.5\,\mathrm{mm} \times 3.5\,\mathrm{mm}$ plus a guard ring on front and back side. In order to resolve single waveforms at high particle rates the sensors are hooked up to a fast, low-noise amplifier with a rise time of approximately 5 ns which was custom built at Ohio State University (OSU). The resulting waveforms are then read out with a DRS4 Evaluation Board at a sampling frequency of 2 GHz. The final diamond pad detectors are then brought into a beam telescope based on the CMS pixel readout chips (ROCs) PSI46v2 which provides

Figure 6: Rate Setup

precise tracking with a resolution of $\sim$70 µm as well as a trigger which can be scaled in area to increase the efficiency of the data taking. At the end of the telescope sits a scintillator as additional trigger to achieve a precise timing of 1 ns. The full setup is shown in figure 6.
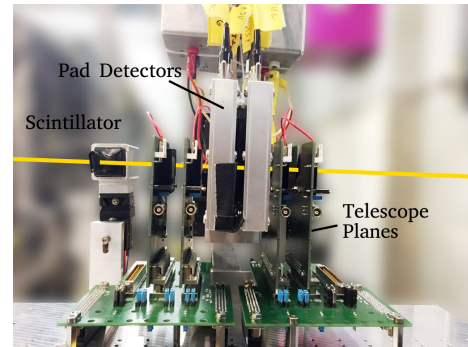
An overlay of 30000 resulting waveforms is shown in figure 7 on the following page. The most dominant peak at 70 ns relates to the actual particle which was triggered on and is called signal region. All the other peak are secondary particles from other bunches. Due to the good timing res-

olution the bunch spacing of the PSI beam can be clearly seen in the plot. The bunch just before the signal region is forbidden by the trigger logic. Therefore there are no peaks in this area and it is used to extract the pedestal (base line) of the waveform. The pulse height value is then calculated by the an integral with a range of 4 ns before and 6 ns after the maximum value in the signal region. The optimisation of the integration window was done by choosing the best Signal to Noise Ratio (SNR).
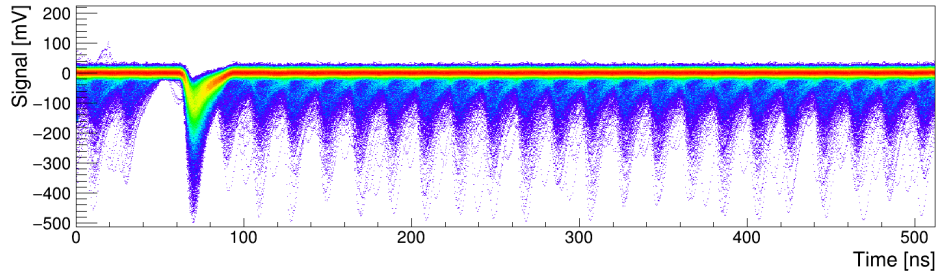

Figure 7: 30000 pCVD diamond waveforms

In order to check the dependence on the incident particle flux several rate scans with both bias voltages and different irradiation doses were performed. The typical scan was starting at the minimum flux, going up to maximum flux with 4 to 5 steps in between (up scan) and then going down to the minimum flux again (down scan). Several of the up and down scans were done in succession to check for long time effects. Figure 8 shows the final results for a pCVD diamond both non-irradiated and irradiated to 5×10^{14} n_{eq}/cm^2. As shown, no pulse height dependence on particle flux was observed for a flux up to $10\,MHz/cm^2$. In addition it can also be seen that there is a slight difference between positive and negative bias. After the irradiation the pulse decreases due to the radiation damage but the values have no absolute calibration yet.
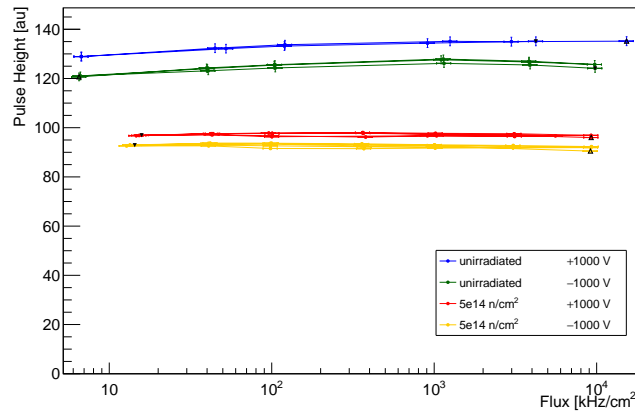

Figure 8: Pulse height versus incident particle flux for a pCVD diamond

5. 3D Detectors

The radiation damage created by HL-LHC will become a big challenge for the innermost

6

tracking detectors. After a large irradiation, all detector material will become trap limited with a MFP below 75 μm. The concept of a so called 3D-Detector is a possible way to highly increase the longevity of these materials. Its basic principle is shown in figure 9: In a planer detector the readout and bias electrodes are brought onto the front and back side of the sensor with a thickness Δ. The resulting drift distance L of the charge carriers is of the order of Δ. In the 3D detector the electrodes are put inside of the detector material so that the MIPs can travel the same distance Δ in the material and therefore create the same amount charge carriers but L is heavily reduced. In case of diamond these electrode columns are drilled with a 800 nm femtosecond laser which converts the diamond into a resistive mixture of carbon phases.

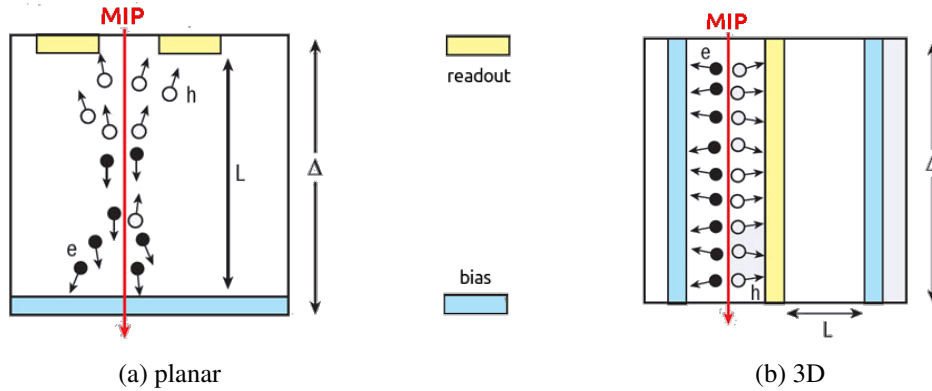(a) planar   (b) 3D

Figure 9: Comparison of the planar and the 3D detector concepts

In 2015 one of the first detectors was built out of a pCVD diamond sensor which had a 3D detector as well as a strip detector on the same sensor. At this time the column efficiency was about 92 % and the 3D cells had a size of 150 μm × 150 μm. This detector was already a success by showing a working 3D diamond detector. Its square cells are clearly visible and the measured signal for the thickness of 500 μm was 13 500 e which is much higher than 6900 e in the strip detector. The strip signal equates to a CCD of 192 μm. The measured charge in the 3D would have a CCD in a planar detector of 350 μm to 375 μm which effectively means that more than 75 % of the created charge was collected for the first time in a pCVD diamond. The according pulse height distributions are shown in **??** on page ??.

6. Conclusion

List of Acronyms

ROC readout chip

LHC Large Hadron Collider

HL-LHC High Luminosity LHC

PSI Paul Scherrer Institut

HIPA High Intensity Proton Accelerator

DUT device under test

SPS Super Proton Synchrotron

MIP minimum ionising particle

CVD Chemical Vapour Deposition

pCVD poly-crystalline Chemical Vapour Deposition

sc single-crystal

p poly-crystalline

BCM Beam Condition Monitor

BLM Beam Loss Monitor

DBM Diamond Beam Monitor

ToF time-of-flight

IP interaction point

CCD charge collection distance

MFP mean free path

OSU Ohio State University

SNR Signal to Noise Ratio

References

[1] G Apollinari, I Béjar Alonso, O Brüning, M Lamont, and L Rossi. *High-Luminosity Large Hadron Collider (HL-LHC): Preliminary Design Report*. CERN Yellow Reports: Monographs. CERN, Geneva, 2015.

[2] Georg Auzinger. Upgrade of the CMS Tracker for the High Luminosity LHC. Technical Report CMS-CR-2016-268, CERN, Geneva, Oct 2016.

[3] F. Bachmair, L. Bäni, P. Bergonzo, B. Caylar, G. Forcolin, I. Haughton, D. Hits, H. Kagan, R. Kass, L. Li, A. Oh, S. Phan, M. Pomorski, D.S. Smith, V. Tyzhnevyi, R. Wallny, and D. Whitehead. A 3d diamond detector for particle tracking. *Nuclear Instruments and Methods in Physics Research Section A: Accelerators, Spectrometers, Detectors and Associated Equipment*, 786:97 – 104, 2015.

[4] Felix Caspar Bachmair. *CVD Diamond Sensors In Detectors For High Energy Physics*. PhD thesis, Zurich, ETH, 2016.

[5] E. Bartz, J. Doroshenko, V. Halyo, B. Harrop, D.A. Hits, D. Marlow, L. Perera, S. Schnetzer, and R. Stone. The plt: A luminosity monitor for cms based on single-crystal diamond pixel sensors. *Nuclear Physics B - Proceedings Supplements*, 197(1):171 – 174, 2009. 11th Topical Seminar on Innovative Particle and Radiation Detectors (IPRD08).

[6] Matevz Cerv. The atlas diamond beam monitor. 9:C02026, 02 2014.

[7] Wim de Boer, Johannes Bol, Alex Furgeri, Steffen Müller, Christian Sander, Eleni Berdermann, Michal Pomorski, and Mika Huhtinen. Radiation hardness of diamond and silicon sensors compared. *physica status solidi (a)*, 204(9):3004–3010, 2007.

[8] M. Domke, C. Ilgner, S. Kostner, M. Lieng, M. Nedos, J. Sauerbrey, S. Schleich, B. Spaan, and K. Warda. Commissioning of the beam conditions monitor of the lhcb experiment at cern. In *2008 IEEE Nuclear Science Symposium Conference Record*, pages 3306–3307, Oct 2008.

[9] elementsix - industry leading engineers. `https://e6cvd.com`, 2017.

[10] A. Goriŝek, V. Cindro, I. Dolenc, H. Frais-Kölbl, E. Griesmayer, H. Kagan, S. Korpar, G. Kramberger, I. Mandi, M. Meyer, M. Miku, H. Pernegger, S. Smith, W. Trischuk, P. Weilhammer, and M. Zavrtanik. Atlas diamond beam condition monitor. *Nuclear Instruments and Methods in Physics Research Section A: Accelerators, Spectrometers, Detectors and Associated Equipment*, 572(1):67 – 69, 2007. Frontier Detectors for Frontier Physics.

[11] Ii-vi incorporated : A global leader in engineered materials and optoelectronic devices and components. `http://www.ii-vi.com/`, 2017.

[12] H Pernegger, V Eremin, H Frais-Kölbl, E Griesmayer, H Kagan, S Roe, S Schnetzer, R Stone, W Trischuk, D Twitchen, Peter Weilhammer, and A Whitehead. Charge-carrier properties in synthetic single-crystal diamond measured with the transient-current technique. *J. Appl. Phys.*, 97(7):73704–1–9, 2005.

[13] Shu-lai Zhao. *Characterization of the electrical properties of polycrystalline diamond films*. PhD thesis, Ohio State U., 1994.